Process-structure-properties in Polymer Additive Manufacturing via Material Extrusion: A review

G. D. Goh, Y. L. Yap, H. K. J. Tan, S. L. Sing, G. L. Goh, W. Y. Yeong*

Singapore Centre for 3D Printing, School of Mechanical and Aerospace Engineering, Nanyang Technological University, 50 Nanyang Avenue, Singapore 639798

*Corresponding Author

Designation: Assistant Professor, School of Mechanical and Aerospace Engineering and Programme Director, Aerospace and Defence Programme, Singapore Centre for 3D Printing, Nanyang Technological University, Singapore

Email: WYYeong@ntu.edu.sg

Tel: 67904343

Abstract

This article provides a database of the mechanical properties of additively manufactured polymeric materials fabricated using material extrusion (e.g., fused filament fabrication (FFF)). Mechanical properties available in the literatures are consolidated in table form for different polymeric materials for FFF. Mechanical properties such as tensile, compressive, flexural, fatigue and creep properties are discussed in detail. The effects of printing parameters such as raster angle, infill, and specimen orientation on properties are also provided, together with a discussion of the possible causes (e.g., texture, microstructure changes, and defects) of anisotropy in properties. In addition to that, research gaps are identified which warrant further investigation.

Keywords: Additive manufacturing, 3D printing, material extrusion, Polymer, mechanical properties

1. Introduction

Fused filament fabrication (FFF) is an additive manufacturing technique which is suitable to produce parts with intricate internal shapes. An FFF printer is essentially a computer numerically controlled (CNC) gantry machine, equipped with one or multi-extruder nozzle head. In the dual-nozzle systems, one of the nozzle is for the modelling material and the other can be for another modelling material or for support material which can either be easily breakable or soluble in alkaline solutions. In FFF technique, parts are manufactured by melting and extruding polymeric filament through a heated nozzle in a prearranged pattern onto a base plate.[1] While the thermoplastic filament is deposited, it cools down to the chamber temperature, gets hardened and fuses with the neighbouring material. After one layer of patterning and depositing, the base plate moves down or the print head moves up before the next layer begins. The process is fully automated and does not need much manpower, making it progressively adopted to produce customized products in different fields.

An important characteristic of the FFF technique is its ability to manufacture objects with functionally graded properties (porosity, density and mechanical properties). With progresses in materials and technology, FFF is shifting from producing prototypes to manufacturing end products. In order for FFF to fully develop into production tool instead of just a machine for prototyping, the mechanical properties of the parts manufactured should be improved such that the performance of the fabricated parts is preserved during service. Apart from that, there should be more variety of polymers that can be used in the FFF technology.

Recently, there have been a lot of research in FFF process optimization as well as development of new materials for FFF technology. In process optimization, extruder temperature [2], raster angle,[2-7] layer thickness,[3, 6, 7] raster gap,[2, 3, 6, 7] raster width,[2, 3, 6, 7] contour width,[6] and specimen orientation[3, 7, 8] are the process parameters that have been studied extensively to obtain the highest possible mechanical properties (Figure 1). Other factors such as filament quality and environmental factors such as oxygen content,[9] temperature[10] and humidity[10, 11] are known to have effect on part quality and mechanical properties. For instance, Lederle et al. observed an increase in elongation at break for amorphous material like ABS and a 30% improvement in tensile strength for polyamide under the absence of oxygen.[9] Halidi and Abdullah noticed that the diameters of the ABS filament feedstock would increase as it absorbs moisture.[11] However, the effect of change in diameters as a result of increase in *et al.* moisture content on the print quality or mechanical properties were not determined. Chuang *et al.* argued that entrapped moisture in the filament will undergo expansion at elevated temperature and thus increases the porosity within the filament which results in lower mechanical properties.[12] Kim et al. noted that FFF-fabricated samples generally absorb more moisture (5-8%) as compared to injection moulded samples (0.34%) and samples with more moisture content perform poorer by as much as 10% in terms of tensile strength.[10] In the same study, they found out that the tensile strength is reduced by about 27% whereas the strain increases when the specimens are at a 60 ^{o}C as compared to room temperature. Materials used for the FFF technology are normally pure thermoplastics such as ABS, PC, Ultem, Nylon, PEEK etc. Composite materials have also been developed to be used in the FFF technology by adding short fibers into the thermoplastics to obtain better mechanical strength. Various static and dynamic mechanical tests have been conducted to assess the suitability of the FFF-printed materials for end-product applications.

Recent review of FFF process focused on the process design and the modelling of FFF technology,[13] the assessment of dimensional accuracy and surface roughness, along with the influence of process

parameters on these important part qualities[14, 15] and different optimization techniques and design of experiments (DOEs) used to optimize the printing process.[16] However, there is no systematic compilation of the mechanical properties of the FFF-printed materials. In this paper, the available data on mechanical properties of materials manufactured by FFF will be systematically reviewed.

Process parameters of FFF

In this section, the definitions of the process parameters will be introduced with the help of illustration as shown in Figure 2.[7, 17]

Layer thickness [mm]: Is the height of each slice of the 3D printied part

*Raster angle [*degree]: Is the angles at which the nozzle deposits molten thermoplastics line-by-line for each layer and it ranges from 0° to 180°.

Contours/shell perimeters: Is the outermost shells to use for the exterior skin and internal hole of the part. The number of the contours/shell perimeters and the contours width can be used to vary the shell thickness.

Raster/bead width [mm]: refers to the width of the extruded filament.

Air/raster gap [mm]: refers to the opening between two adjacent extruded filaments, and, a negative air gap means there is overlapping between two adjacent filaments.

Deposition speed [mm/min]: It is the speed at which the nozzle moves. This is directly related to printing speed.

Fill Density [%]: The amount of material within the part. The higher the percentage of fill, the better the mechanical properties of the part, however, the printing time will be longer and more material will be needed.

Platform/bed Temperature [°C]: It is the temperature of the build platform. This parameter determines the cooling rate of the extruded filament especially on the first layer and is an important parameter for good adhesion of the first layer and the prevention of warping effect.

Nozzle Temperature [°C]: This is the temperature at which the material is being extruded. The temperature is normally a few degrees Celsius higher than the melting point of the materials.

Chamber Temperature [°C]: Some FFF printers have controlled temperature environment to have a more consistent printing result. This refers to the ambient temperature inside the build environment.

Specimen/Build orientation denotes the direction of the printed part on the build platform, about the *x*, *y* and *z*-axes.

Mechanical properties of additively manufactured polymeric materials

Review of the literature shows that significant amount of the published work has concentrated on tension and flexural testing. Other tests such as compression and fatigue testing are also available. In the tables, the effects of specimen orientation and printing parameters such as raster angles and layer thickness on various mechanical properties are reported. The X, Y, Z labels used for the specimen orientation shown in Figure 3 are in accordance with the standard (ISO/ASTM 5291:2013 Standard Terminology for Additive Manufacturing – Coordinate Systems and Test Methodologies) and have been used by Lewandowski et al. to systematically discuss the mechanical properties of the AM metal parts.[18] As stated in the standard, Z denotes the build direction. The X axis is parallel to the front of the machine and is perpendicular to Z.

The Y axis is normal to both the Z and X axes, with a positive direction defined to make a right-hand set coordinates. For rectangular and unsymmetrical test specimens, three letters (X,Y,Z) are needed to define the orientation. The first letter denotes the axis parallel to the longest overall dimensions. The second letter denotes the second-longest overall dimension, while the third letter denotes the shortest dimension of the coupon. As an illustration, a specimen with XYZ designation means that its longest dimension is aligned to X axis, its second-longest dimension is aligned to Y-axis, and its shortest overall dimension is aligned to Z-axis.

Quasi-static properties: tensile, compression, flexural, hardness and fracture toughness

Thus far, various tests have been used to determine the tensile, compression, flexural, hardness, and fracture toughness of the polymer materials. Tensile properties are the most commonly used properties by researcher to determine the material properties. Hence, in this section, tensile properties of different materials produced using FFF technique will be discussed in depth. Based on available information, other mechanical properties will also be discussed.

Tensile properties

Table 1 is a compilation of published tensile properties for various materials fabricated using FFF along with literature references. In addition to that, Table 2 shows the machine types and materials used; shows the testing standard and dimension of the specimens used; and specifies whether the specimen is tested in as-built or thermal-treated condition.

Dependence of mechanical properties such as ultimate tensile strength (UTS), elastic modulus, and elongation to failure on printing parameters such as raster angle and specimen orientation is observed. Generally, 0^{o} raster angle gives the highest UTS and elastic modulus.[5, 19-22] The

UTS and elastic modulus drop as the raster angle increases until 90 ^{o}. This is because changing raster angles affect how load is transferred within the specimens. When the raster angle increases, the bonding between adjacent filaments (intra-layer bond (Figure 4A)) play a bigger role in carrying the load.[23] The variation with respect to raster angle suggests that bonding of polymer between the adjacent filament is not as strong as bonding of polymer within the filament. The poorer bonding could be attributed to the inadequate fusion of polymer chains at the boundary between the adjacent filaments as a result of the fast cooling nature of the printing technique. Due to the inadequate fusion at the boundary, each extruded filament can be treated as a fiber which can take higher stress in the fiber direction and lowest stress perpendicular to the fiber direction.

The effect of raster width on the tensile properties is divisive. Onwubolu and Rayegani[7] found that smaller raster width would result in higher tensile strength. However, the results are the opposite in the studies by Sood *et al.*[3] and Alhubail[6] in which higher tensile strength is obtained with larger raster width. More in depth research would be needed to conclusively determine the effect of raster width on the tensile properties.

Apart from that, the anisotropy of mechanical properties is affected by the specimen orientation. Specimen printed in XYZ and XYZ orientations generally provides better mechanical strength compared to ZXY orientation.[19, 24, 25] The tensile strength and the elongation in the ZXY orientation is normally 40-50% of the tensile strength and elongation respectively in XYZ and YXZ orientations. The reason for the deviation was due to the different failure modes that specimens of different orientations exhibit. For the ZXY orientation, the specimens are pulled

in the across-the-layer direction and the load is normal to the fibres direction, leading to inter-layer fusion bond (ILFB) failure.

In the ZXY orientation, interlayer or fibre-to-fibre bond (Figure 4A) greatly influences the tensile strength. This is because the fibres do not take the applied load, instead, ILFBs between adjoining layers bears majority of the pulling force. As far as the YXZ and XYZ orientations printed tensile coupons are concerned, they are pulled in the in-plane directions and the fibres are stressed, leading to trans-layer failure. Here, the fibres bear majority of the pulling force and fibre breakage would normally be observed. Interestingly, the elastic modulus is least affected by the specimen orientation. The maximum percentage deviation of the elastic modulus in the three orientations is only about 18%.[25]

Layer thickness (Lt) is a highly disputed parameter due to variation in the results from different research groups. Rankouhi *et al.*[26] stated that even though layer thickness has been investigated widely, more detailed investigations should be carried out owing to the discrepancy of results. For instance, Sood *et al.*[3] found out that tensile strength first dropped and eventually rose with increasing layer thickness from 0.127 mm to 0.178 mm, and to 0.254 mm. Another research group compared two layer thicknesses (0.2mm and 0.4mm) of acrylonitrile butadiene styrene (ABS) and polylactic acid (PLA) specimens and concluded that lower thickness produced higher tensile strength.[27] However, PLA specimens exhibited larger variability between parameters. Similar results have been shown by Vaezi and Chua[28] in which a decrease in layer thickness would favour the enhancement of tensile properties. It was found that increasing number of shell perimeters would lead to higher disparity of tensile strength with layer thickness.[17] Onwubolue *et al.* concluded that maximum tensile stress is achieved by using minimum layer thickness.[7] A more detailed study on the effect on layer thickness on the

mechanical properties of the FFF printed parts at different specimen orientations revealed that the effect of layer thickness and the specimen orientation are coupled in determining the tensile properties of FFF-printed parts.[25] It was found that the tensile strength increases for the specimens in XYZ direction as the layer thickness decreases. The opposite trend is observed for the specimens in ZXY orientation.

The feed rate/ printing speed is an important parameter as it is associated with printing time, and therefore, to production cost. The higher feed rate allows parts to be printed faster and thus increasing productivity. However, the feed rate cannot be increased indefinitely as it also has an effect on the tensile properties. For instance, the studies of Ning *et al.*[29] and Christiyana *et al.*[30] have revealed that tensile strength dropped as the feed rate increased. It was also found that the significance of the feed rate is dependent on the specimen orientation. Feed rate plays an important role when the specimen is in ZXY orientation. The tensile strength increases when the feed rate decreases. However, the effect of feed rate on the tensile strength is not significant in the XYZ and XYZ orientations.

In FFF, when the layer thickness is larger or printing speed is higher, the lesser the overall degree of cooling on the deposited filaments.[31] Higher average temperature of the deposited filament is essential for inter-layer fusion which in turn gives rise to higher mechanical properties in across-the-layer direction. Due to this, higher layer thickness, which usually has lower cooling rate due to higher heat capacity of the extruded filament (due to higher mass of the extruded filament), usually associates to higher mechanical performance in across the layer direction.[32] Inter-layer cooling time is found to be inversely related to tensile properties of FFF-printed parts,[33] i.e., the lower the printing speed, the longer the inter-layer cooling time. A longer interlayer cooling time allows the just-deposited material to be cooled down to the

chamber temperature, which normally is lower than the glass transition temperature of the material. This lower temperature disfavours the fusion of the thermoplastics at the interlayers. As the samples in ZXY orientation are loaded in the across-the-layer direction, and hence their strength and ductility are affected by the interlayer cooling time. The XYZ specimens, contrarily, are not loaded in the across-the-layer direction, and hence are not directly influenced by interlayer cooling time.

Infill pattern and infill percentage are two parameters that are available in FFF technique to save materials.[34] The lower the infill percentage, the lesser the material is used, thus saving cost and reducing weight of the part. However, at the same time, the mechanical properties will be compromised as lowering the infill percentage also means introducing voids inside a part. Numerous studies have been conducted in relation to the infill pattern and infill percentage of the printed parts.[35] It was found out that the fill pattern has negligible effect on the mechanical properties of the FFF-printed parts.

Apart from printing parameters and choice of materials, there are other factors that would affect the resulting mechanical properties. For instance, the mechanical properties of the AM materials are dependent on the how fast the load is applied in the tensile test, i.e. the measured UTS and elastic modulus are found to be higher at lower strain rate. It should be noted, however, that due to the variation in gauge length used by different researchers, direct comparison of elongation to failure should be avoided. In addition to that, variation in the type and quality of the polymer filament is found to affect the resulting mechanical properties. Tymrak *et al.* noticed that the filaments of different colours would give different extrusion characteristics, even though they are from the same manufacturer.[27] In general, the reported tensile properties of the AM polymeric materials are found to be slightly lower than those conventionally manufactured polymers. The lower mechanical properties are attributed to presence of voids in

the additively manufactured specimens (Figure 5). Voids can be reduced by applying negative raster gap and thus better mechanical properties can be achieved.[36] In processing process such as infrared preheating[37] or laser-assisted heating[38] were introduced to improve the mechanical performance of the parts. Post treatment process such as thermal treatment could help improve the tensile properties by improving bonds between adjacent filaments (for FFF).[39] Improvement in tensile properties after the thermal treatment has been reported. But most importantly, precise control of FFF process parameters like printing speed and particularly build platform and the environment temperatures can avoid such problem during the fabrication process.

Compressive properties

A compression test is able to determine the material behaviour under a quasi-static crushing load. As compression test cannot be considered significant for typical engineering design perspective, limited data and articles have reported on the compressive properties of FFF printed specimens. The compressive strength is regarded as meaningless in the case when the material does not fail in compression by a shattering fracture as the polymer materials will continue to deform until it is flattened completely, resulting in the compressive stress to increase steadily during compression tests. The most commonly used standard test method for compression test is the ASTM D695 - Standard Test Method for Compressive Properties of Rigid Plastics. Various forms of specimens, for example, sheet, plate, rod and tube, can be used based on the material specifications and thickness. The speed of testing is usually 1.3 ± 0.3 mm/min, as suggested by the ASTM standard.

Build orientation has a substantial impact on the compressive strength. Compression specimens built in the Z-orientation generally produce a higher compressive strength then those built in the X-orientation.[40-42] The difference in compressive strengths of the two orientations is due to the fact that to the layers are arranged normal to the acting load, leading to increased compressive strength in the Z-orientation specimens.[42]

Raster angle is also one of the important parameters that affects the compressive properties of FFF printed specimens. Single raster orientation angle specimens have consistent clean fracture due to buckling while alternating raster orientations ($0^o/90^o$) specimens fail in a more complex and inconsistent manner. In the study by Krishna *et al.*, [40] it was found out that different raster angles ($0^o/90^o$ and $45^o/-45^o$) produce different compressive yield strength on the X-orientation specimens, but not on the Z-orientation specimens. This is because in the case of the Z-orientation specimens, the internal structure is essentially the same for resisting the applied load that is perpendicular to the area of the raster. But for the X-orientation specimens, the $0^o/90^o$ raster offers stronger resistance against deformation as compared to $45^o/-45^o$ specimens. However, Zieman *et al.*[5] reported that 45^o raster specimens exhibited poorer compressive properties while other raster angles produced similar compressive strength. This is due the distortion as a result of shearing along the 45^o rasters when the specimen was compressed.

Compressive properties of FFF fabricated specimens are still very limited and hence the effects of other parameters such as layer thickness and infill pattern are not covered at current stage.

Flexural properties

Flexural test is the second most common quasi-static mechanical test conducted to get the knowledge of how the materials behave under bending loads. The available information on the flexural properties is significant lesser as compared to the tensile properties. The FFF-printed

materials that has been tested for flexural properties are ABS, PEEK, Nylon, and PLA. Thus far, three-point bending test is the only method to get the flexural data and ASTM D790 Standard Test Methods for Flexural Properties of Unreinforced and Reinforced Plastics and Electrical Insulating Materials is the most commonly used standard for the three-point bending test although ISO 178:2001 Plastics - Determination of flexural properties has also been used to test the flexural properties. It is interesting to note that another standard test method, ASTM6272 - Standard Test Method for Flexural Properties of Unreinforced and Reinforced Plastics and Electrical Insulating Materials by Four-Point Bending – has not been used to determine the flexural properties of FFF-printed materials to the authors' knowledge. The reason for not using the four-point bending test could be due to the need for extra instrument to determine the maximum deflection at the center of the test coupon. Although the researchers used the same standard for the flexural test, the specimen dimensions and the strain rates differ resulting in deviation in the data obtained from the flexural test. It is evident in [25] and [22] that although both groups used PLA as the material of study, the differences in specimen dimensions and strain rates resulted in the disparity in the results.

Similar to tensile properties, it was found that printing parameters such as specimen orientations, raster angle, and layer thickness affect the flexural properties of FFF-printed materials. Anisotropy in flexural properties was observed in FFF-printed materials. The maximum flexural strength and stiffness were observed in YXZ orientation and were followed by XYZ orientation and then ZXY orientation. Specimens in the YXZ are the strongest because the load is acting across the intralayer bond between the adjacent filament in the YXZ specimens. On the other hand, load is acting across interlayer bond between adjacent layers in the XYZ specimens. As noted in the tensile section, intralayer bond would be stronger than the interlayer bond due to the better fusion of the adjacent filament as a result of the lower

temperature drop of the deposited filament. The ZXY specimens exhibit the lowest flexural strength as the load is applied in the direction such that the fibres do not bear the load, instead, interlayer fusion bonds between adjacent layers or fibres bear majority of the pulling force.

Raster angle also plays a part in determining the flexural properties of the FFF-printed parts. In general, 0 ^{o} raster angle is the strongest and the strength decreases as the raster angles increases to 90^{o}. The effect of raster angle on flexural properties can be explained from the failure mode of the flexural specimens. When a flexural specimen is loaded, one side will experience compression while the other side will experience tension. As observed from the Table 1 and Table 3, the tensile strengths of the thermoplastic materials are lower than their compressive strength. This means that the tensile side of the specimen will fail first and thus the tensile properties are the determining factors of the flexural properties. As the UTS of the thermoplastics is affected by the raster angle, and thus the flexural properties are also a function of raster angle.

Layer thickness has a dominant, statistically significant effect on flexural force.[43] However, the layer thickness has different effect on specimens of different orientations. For XYZ specimens, flexural strength is the highest when layer thickness is lowest. For ZXY specimens, the flexural strength is the highest when the layer thickness is highest.

In general, the flexural properties are strongly influenced by the printing parameters such as specimen orientations, raster angles, and layer thickness. However, the effect of infill pattern on the flexural properties has not been extensively studied.

Interlayer properties

Table 4 is a compilation of published interlayer properties for various materials fabricated using FFF. In addition to that, Table 4 also shows the sample design, printing parameters, testing

parameters. Thus far, three different properties have been used to gauge the interlayer properties of the FFF-fabricated polymer parts, they are the ZYX and ZXY-directions tensile strength, interlayer fracture toughness and interlaminar shear properties. The interlayer properties have been compared with that of the polymers fabricated using conventional processes. It was found that the mode I interlayer fracture toughness of the FFF-fabricated polymer parts was lower when compared with compression moulded polymer parts.[44] The lower mode I interlayer fracture toughness was found to be caused by the presence of pores at boundary between the extruded filament. The presence of pores in the printed parts is a common characteristic of FFF-fabricated parts which can be minimized by using negative raster gap. Other than that, the investigation on the effect of the addition of reinforcements to the polymers on the interlayer properties has also been conducted. A drop in the interlayer properties has been observed when fibre reinforcements were added. For instance, the ZYX and ZXY-directions tensile properties of the carbon fiber-filled ABS is only 42% of that of the pure ABS.[45] Apart from that, another study has shown that the interlayer fracture toughness of the carbon fiber-filled ABS is about 5 times lower than that of the pure ABS.[44] Another study showed that the interlaminar shear strength of the reinforced ABS is 8.5 times lower than that of the pure ABS.[46] This suggests that the strengthening of the in-plane properties by the addition of reinforcement comes at the expense of poorer interlayer properties. This is because the addition of reinforcement reduces the amount of bond formation of the thermoplastics at the interlayer boundary (Figure 4B). Although some work to improve the interlaminar properties of pure thermoplastics has been going on such as in-process laser heating,[47] more research is needed to improve the interlayer bond of the reinforced thermoplastics.

Dynamic properties: Creep, fatigue and crack growth

As discussed above, the existence of process induced defects and variation in microstructures as a result of difference in printing parameters would affect the tensile and interlaminar properties. The variation in microstructures as a result of difference in printing parameters will also affect the cyclic behaviour of the FFF-fabricated polymer parts.

Fatigue properties

Fatigue testing is able to determine the number of cycles a plastic material can take given a certain load. The test can be done in the uniaxial direction or along the cross section. The load applied on the plastic should be within the elastic region. Thus far, standards such as UNI EN ISO 527-1 (1997) Determination of Tensile Properties of Plastics, ASTM D7791- Standard Test Method for Uniaxial Fatigue Properties of Plastics, ASTM D7774-12- Standard Test Method for Flexural Fatigue Properties of Plastics, ASTM D4482 - 11 - Standard Test Method for Rubber Property—Extension Cycling Fatigue have been used to test the fatigue properties of the FFF-fabricated thermoplastic parts.

As shown in table 5 is the compilation of fatigue properties of various polymers fabricated using FFF. In order to make a reasonable comparison of the fatigue properties, all data from various sources have been fitted with linear lines using the formula, $S = A\log(N) + B$, where S is the stress, N is the number of cycles, A is the gradient of the slope and B is the y-intercept which corresponds to the max stress at static load. However, it must be mentioned that different standards have been used to obtain the fatigue properties which may result in data not being directly comparable among the studies. Nevertheless, there are still some printing parameters such as printing direction and raster angles that can be discussed.

Build orientation has a significant impact on the fatigue life. Coupons printed in the Z-orientation had significantly lower strain capability for a given number of cycle.[48, 49] The

difference can be due to weaker bonds in-between layers causing lower fatigue life when loads are applied parallel to the build direction. Apart from that, specimens printed in YXZ orientation are able to resist higher initial cyclic loading and exhibit lower drop in strength after 10000 cycles when compared to specimens in XYZ orientation (Figure 6).[48] Raster angle was also found to have some difference in fatigue life with 90 degrees rotation having the lowest fatigue life and 45 degrees having the largest.[22] It should be noted that the difference is approximately around 10MPa at the one millionth cycle, which may not be significant depending on application. Different failure modes were observed in cross-ply bidirectional and unidirectional specimens. For cross-ply bidirectional specimens, the fatigue failure occurs in three stages which is not observed in unidirectional specimens. At the first stage, the fatigue crack propagates at a high rate due to the appearance of multiple damage modes, such as crazing,[21, 48] fiber cracking, delamination,[21] void geometry changes.[50] In the second stage, the cracks propagate at a steady and lower rate. In the last stage, the cracks speed up due to fiber fracture.[50]

Infill density and pattern was found to have effects on the fatigue performance of the FFF-fabricated parts.[51] Honeycomb infill pattern was found to have a longer lifespan compared to a rectilinear infill pattern with similar infill density.

Other printing parameters such as the layer thickness and nozzle diameter have been found to be important in influencing the fatigue performance.[51, 52] Larger layer thickness and nozzle diameter would generally result in better fatigue performance. However, the layer thickness cannot be increased indefinitely as it will have adverse effect due to improper bonding between the layers. It has been recommended that a minimum of 1:1.5 ratio between layer thickness and nozzle diameter should be kept.

Creep properties

Creep is a time-dependent mechanical property which determines the slow deformation of the solid materials under constant mechanical loading. It gives an idea about the long-term durability and reliability of a material under continuous loading which are important especially in automotive and aerospace industries as it affects the safety of the FFF-manufactured parts. Creep study of the FFF-fabricated parts is very limited. Thus far, there are only four studies have been found to be related to creep deformation. The relationship between the FFF process and the creep properties has been developed by Mohamed *et al.*[53, 54] PC-ABS blend material was used in the study. However, the test was carried out at single stress and single temperature. D. Türk *et al.* studied the flexural creep modulus of the FFF-fabricated materials (ABS, Polyamide 12) at various temperatures and at two different specimen orientations through three-point bending creep tests.[55] It was found that the specimen orientation has an effect on the flexural creep modulus for ABS, but not for PA-12.[55] For ABS, the flexural modulus of the XYZ specimens (2200 MPa) was found to be slightly higher than that of the ZXY specimens (2050 MPa). In the experiment by Salazar-Martín *et al.*,[56] the number of contours was found to be inversely related to the creep strain with raster angle being set at 45º. This shows the significance of the direction of the deposited filaments in the specimens relative to the direction of the puling force. It is evident in the creep test of different specimen orientations, where XZY/YZX specimens were found to be more creep-resistant than XYZ/YXZ specimens, that the number of contours plays a significant role in resisting the creep.[56] This is due to the fact that XZY/YZX specimens have higher percentage of contours as compared to XYZ/YXZ specimens making it able to resist creep better. Apart from that, changing the density by varying the raster air gap was also found to affect the creep resistance. Besides, Layer thickness and raster angle were found to play critical roles in the creep performance of the FFF-fabricated

parts. Increasing layer thickness from 0.127 mm to 0.3302 mm and raster angle from 0° to 90° were found to have negative impact on the creep performance.[57] In general, XZY/YZX specimen orientations, smaller layer thickness, zero raster angle, zero airgap and maximum number of contours will give the most optimum creep properties.

Potential

There is an increasing effort to inspect, compensate, and improve the quality of the parts fabricated using FFF. In this section, the latest trend in improving, checking and compensating for mechanical properties of FFF-fabricated parts are discussed.

Topology optimization

Much effort has been made to incorporate additive manufacturing with topology optimization. In order to achieve this, topology optimization software must be able to take into account of the anisotropy of the FFF-fabricated parts in its algorithms. Also, Topology optimization often results in design that are complex and not FFF friendly. For instance, topologically optimized designs may need a lot of support structures to be fabricated using FFF, resulting in prolonged fabrication time and post-processing costs.[58] Some effort has been made to take into consideration of the printing technique by restricting the generation of overhanging structures and it eliminates the need of sacrificial support materials, thus saving time and money.[59]

Standardization of test methods

Additionally, the lack of standards has caused the results generated by different research groups not directly comparable due to the difference in testing methods. More stringent control over the testing parameters is needed so that only one commonly accepted standard is adopted by

the research community to ensure consistency in the published works. In 2013, ISO and ASTM worked together to develop one set of global standards containing general standards that are relevant to most AM materials, processes, and applications; which includes the standards for testing of materials.[60] This is crucial for establishing and applying AM-related testing tools and methodologies. For instance, ISO/ASTM DIS 52903 ‘‘Standard specification for material extrusion based additive manufacturing of plastic materials’’ is currently under development[61].

Diagnostic techniques

Non-destructive tests (NDT) are needed to inspect the integrity of the fabricated parts and are crucial for the certification and qualification of the FFF-fabricated parts. The flexibility of FFF to produce parts with intricate geometries poses a challenge for conventional NDT methods such as ultrasonic test, eddy current test, and magnetic particle test. For instance, Zeltmann et al. attempted using ultrasonic C-scan to detect inner defects.[62] However, this test method was not able to identify the defects as large as 500 microns. The most promising NDT technique for intricate shape parts appears to be x-ray computed tomography (CT). Various groups have used CT-scan to acquire information within the FFF-fabricated parts.[63, 64] However, CT still comes with some disadvantages. For instance, CT is not ideal for crack detection, and the scanning process is slow and time-consuming before analysis can be conducted.[65] More work is being carried out to further optimize the existing NDT technique to suit the additively manufactured parts. For instance, ISO/ASTM NP 52905 ‘‘Non-destructive testing of additive manufactured products’’ is currently under development.[66]

In-situ monitoring and control

Defects present in the printed parts can be detrimental to the mechanical properties causing it to fail earlier than expected. Real-time monitoring is crucial for the assessment and control of the printed parts' quality by eliminating the presence of undesirable effects.[67] Ultrasonic inspection has been used to detect faults present in the print by comparing the frequency response to the predetermined ideal frequency response.[68] However, this method only works in solid and simple geometries. In another work, acoustic emission is used to monitor the material loading condition to check if there is any nozzle clogging issue.[69] In-situ monitoring of strain and temperature profile using fiber Bragg grating (FBG) sensors has allowed researchers to study and control the diffusion time of the FFF-extruded thermoplastics.[70] However, this involves pausing the print and inserting the sensor on the last deposited layer. Dinwiddie et al. used an extended range IR camera to do is-situ temperature monitoring of parts fabricated during the FFF process, to study the effect of changes in surrounding temperature on the mechanical properties of the printed parts.[71] Temperature was found to be decreasing rapidly after deposition from 250^{o}C to 60^{o}C in just 8 seconds for ABS materials, leading to thermal stresses and –distortions.[72] Abovementioned techniques are all real-time monitoring without any closed-loop feedback control. Attempts on in-situ control of the FFF technique have also been made. Fang *et al.* developed, developed an in-situ surface quality monitoring system FFF systems, using signature analysis technique. The signature, which is the image grayscales of an ideal layer patterns generated using mathematical modelling, is compared with the image of actual deposited pattern of the same layer captured using camera. The comparison with the ideal layer pattern enables the possibility to detect under- and overfills on a layer and correct these during the production process.[73] Real-time optical monitoring using a two-camera system for FFF has also been conducted by Nuchitprasitchai *et al.* and this technique was able to detect 100% detection rate for failure. Similar study to use image

processing to detect defects has been demonstrated by Straub *et al*.[74] However, these two studies can only detect failure due to loss of filament during the printing process and in-process correction to compensate the defect were not implemented. More research is needed to improve on the early detection of defects of the just deposited layers (which will be later hidden) as it is far more important that post-process (printing) NDT.

Conclusion and future research perspective

In this review, various static and dynamic mechanical tests that normally used to evaluate the mechanical properties of the FFF printed materials are discussed in detail. Tensile, flexural, compressive, and fatigue properties are some of the most common mechanical properties that have been investigated. Nevertheless, properties such as creep, impact resistant,[75-77] and wear resistant[78-80] can also be found with limited available information. Research focus has been on the optimization of process parameters for different thermoplastic materials. However, there is limited information with regards to how cooling rate affects the crystallization of the thermoplastics and eventually the mechanical properties of the FFF printed materials. Thus, much research work is required in this area in the future research.

More research work is warranted in the material development field to widen the choice of materials for FFF technique. The creation of new thermoplastic blends and fibre reinforced thermoplastic composites are some of the effort to develop new properties which are not found in a single polymer. The development of new materials needs to be complemented by the understanding of the physics involved during the deposition process. Modelling of the temperature variation and stress would allow operator to predict the microstructures and mechanical properties resulting from the selected printing parameters. However, due to the fast heating and cooling nature of the process, the melting and recrystallization of the FFF-

fabricated thermoplastics is not fully understood and is hard to be predicted using conventional theories and models. This necessitates the need to have a better understanding on the physics to improve on the quality and mechanical properties of the parts. Efforts have been made to study the heat transfer of the FFF technique[81] and the bond and the coalescence of the filament[82] in attempts to enhance the understanding on the extrusion process. Apart from that, lack of efficient computational tools hindered the effort to translate the high-fidelity models into real-time process control for the FFF technique. Besides, difficulty in acquiring fast and accurate measurements of the temperature, cooling rate, and residual stress is another challenge in the in-process monitoring and control. Lastly, finite element software must be improved by adding composite simulation capabilities with multiscale modelling and inverse design capabilities to facilitate the search in the complex process-structure-property relationships. Figure 7 below shows an integrated approach to designing structural parts. In short, coming up with a predictive model to determine the structural integrity or properties of a FFF-printed parts require a collective effort from several science and engineering disciplines at academic, industrial and government institutions.

Acknowledgement

This research is supported by the National Research Foundation, Prime Minister's Office, Singapore under its Medium-Sized Centre funding scheme.

References

1. Sun, Q., G.M. Rizvi, C.T. Bellehumeur, and P. Gu, Effect of Processing Conditions on the Bonding Quality of Fdm Polymer Filaments. *Rapid Prototyping Journal* **14**, 72-80 (2008).

2. Montero, Michael, Shad Roundy, Dan Odell, Sung-Hoon Ahn, and Paul K Wright, Material Characterization of Fused Deposition Modeling (Fdm) Abs by Designed Experiments. *Society of Manufacturing Engineers* **10**, 13552540210441166 (2001).
3. Sood, A K, R K Ohdar, and S S Mahapatra, Parametric Appraisal of Fused Deposition Modelling Process Using the Grey Taguchi Method. *Proceedings of the Institution of Mechanical Engineers, Part B: Journal of Engineering Manufacture* **224**, 135-45 (2010).
4. Fatimatuzahraa, A. W., B. Farahaina, and W. A. Y. Yusoff. "The Effect of Employing Different Raster Orientations on the Mechanical Properties and Microstructure of Fused Deposition Modeling Parts." Paper presented at the 2011 IEEE Symposium on Business, Engineering and Industrial Applications (ISBEIA), 25-28 Sept. 2011 2011.
5. Ziemian, Constance, Mala Sharma, and Sophia Ziemian. "Anisotropic Mechanical Properties of Abs Parts Fabricated by Fused Deposition Modelling." In *Mechanical Engineering*, 159-80: InTech, 2012.
6. Alhubail, Mohammad. "Statistical-Based Optimization of Process Parameters of Fused Deposition Modelling for Improved Quality." University of Portsmouth, 2012.
7. Onwubolu, Godfrey C., and Farzad Rayegani, Characterization and Optimization of Mechanical Properties of Abs Parts Manufactured by the Fused Deposition Modelling Process. *International Journal of Manufacturing Engineering* **2014**, 13 (2014).
8. Górski, Filip, Wiesław Kuczko, and Radosław Wichniarek, Influence of Process Parameters on Dimensional Accuracy of Parts Manufactured Using Fused Deposition Modelling Technology. *Advances in Science and Technology Research Journal* **7**, 27-35 (2013).
9. Lederle, Felix, Frederick Meyer, Gabriella-Paula Brunotte, Christian Kaldun, and Eike G. Hübner, Improved Mechanical Properties of 3d-Printed Parts by Fused Deposition Modeling Processed under the Exclusion of Oxygen. *Progress in Additive Manufacturing* **1**, 3-7 (2016).
10. Eunseob, Kim, Shin Yong-Jun, and Ahn Sung-Hoon, The Effects of Moisture and Temperature on the Mechanical Properties of Additive Manufacturing Components: Fused Deposition Modeling. *Rapid Prototyping Journal* **22**, 887-94 (2016).
11. Mohd Halidi, Siti Nur Amalina, and Jamaluddin Abdullah, Moisture and Humidity Effects on the Abs Used in Fused Deposition Modeling Machine. *Advanced Materials Research* **576**, 641-44 (2012).
12. Chuang, Kathy C, Joseph E Grady, Robert D Draper, Euy-Sik E Shin, Clark Patterson, and Thomas D Santelle. "Additive Manufacturing and Characterization of Ultem Polymers and Composites." In *The Composites and Advanced Materials Expo CAMX*. Dallas, TX; United States: NASA, 2015.
13. Brian, N. Turner, Strong Robert, and A. Gold Scott, A Review of Melt Extrusion Additive Manufacturing Processes: I. Process Design and Modeling. *Rapid Prototyping Journal* **20**, 192-204 (2014).
14. N., Turner Brian, and Gold Scott A, A Review of Melt Extrusion Additive Manufacturing Processes: Ii. Materials, Dimensional Accuracy, and Surface Roughness. *Rapid Prototyping Journal* **21**, 250-61 (2015).
15. Mohan, N., P. Senthil, S. Vinodh, and N. Jayanth, A Review on Composite Materials and Process Parameters Optimisation for the Fused Deposition Modelling Process. *Virtual and Physical Prototyping* **12**, 47-59 (2017).
16. Mohamed, Omar A., Syed H. Masood, and Jahar L. Bhowmik, Optimization of Fused Deposition Modeling Process Parameters: A Review of Current Research and Future Prospects. *Advances in Manufacturing* **3**, 42-53 (2015).
17. Antonio, Lanzotti, Grasso Marzio, Staiano Gabriele, and Martorelli Massimo, The Impact of Process Parameters on Mechanical Properties of Parts Fabricated in Pla with an Open-Source 3-D Printer. *Rapid Prototyping Journal* **21**, 604-17 (2015).
18. Lewandowski, John J., and Mohsen Seifi, Metal Additive Manufacturing: A Review of Mechanical Properties. *Annual Review of Materials Research* **46**, 151-86 (2016).

19. Weng, Zixiang, Jianlei Wang, T Senthil, and Lixin Wu, Mechanical and Thermal Properties of Abs/Montmorillonite Nanocomposites for Fused Deposition Modeling 3d Printing. *Materials & Design* **102**, 276-83 (2016).
20. Afrose, Mst Faujiya, S H Masood, Pio Iovenitti, Mostafa Nikzad, and Igor Sbarski, Effects of Part Build Orientations on Fatigue Behaviour of Fdm-Processed Pla Material. *Progress in Additive Manufacturing*, 1-8 (2015).
21. Ziemian, Sophia, Maryvivian Okwara, and Constance Wilkens Ziemian, Tensile and Fatigue Behavior of Layered Acrylonitrile Butadiene Styrene. *Rapid Prototyping Journal* **21**, 270-78 (2015).
22. Letcher, Todd, and Megan Waytashek. "Material Property Testing of 3d-Printed Specimen in Pla on an Entry-Level 3d Printer." Paper presented at the ASME 2014 International Mechanical Engineering Congress and Exposition, 2014.
23. Rezayat, H., W. Zhou, A. Siriruk, D. Penumadu, and S. S. Babu, Structure–Mechanical Property Relationship in Fused Deposition Modelling. *Materials Science and Technology* **31**, 895-903 (2015).
24. Domingo-Espin, Miquel, Josep M. Puigoriol-Forcada, Andres-Amador Garcia-Granada, Jordi Llumà, Salvador Borros, and Guillermo Reyes, Mechanical Property Characterization and Simulation of Fused Deposition Modeling Polycarbonate Parts. *Materials & Design* **83**, 670-77 (2015).
25. Chacón, J. M., M. A. Caminero, E. García-Plaza, and P. J. Núñez, Additive Manufacturing of Pla Structures Using Fused Deposition Modelling: Effect of Process Parameters on Mechanical Properties And their Optimal Selection. *Materials & Design* **124**, 143-57 (2017).
26. Rankouhi, Behzad, Sina Javadpour, Fereidoon Delfanian, and Todd Letcher, Failure Analysis and Mechanical Characterization of 3d Printed Abs with Respect to Layer Thickness and Orientation. *Journal of Failure Analysis and Prevention* **16**, 467-81 (2016).
27. Tymrak, B. M., M. Kreiger, and J. M. Pearce, Mechanical Properties of Components Fabricated with Open-Source 3-D Printers under Realistic Environmental Conditions. *Materials & Design* **58**, 242-46 (2014).
28. Vaezi, Mohammad, and Chee Kai Chua, Effects of Layer Thickness and Binder Saturation Level Parameters on 3d Printing Process. *The International Journal of Advanced Manufacturing Technology* **53**, 275-84 (2011).
29. Ning, Fuda, Weilong Cong, Yingbin Hu, and Hui Wang, Additive Manufacturing of Carbon Fiber-Reinforced Plastic Composites Using Fused Deposition Modeling: Effects of Process Parameters on Tensile Properties. *Journal of Composite Materials* **51**, 451-62 (2017).
30. Christiyan, K. G. Jaya, U. Chandrasekhar, and K. Venkateswarlu, A Study on the Influence of Process Parameters on the Mechanical Properties of 3d Printed Abs Composite. *IOP Conference Series: Materials Science and Engineering* **114**, 012109 (2016).
31. Zhang, Jie, Xin Zhou Wang, Wang Wang Yu, and Yu He Deng, Numerical Investigation of the Influence of Process Conditions on the Temperature Variation in Fused Deposition Modeling. *Materials & Design* **130**, 59-68 (2017).
32. Carneiro, OS, AF Silva, and Rui Gomes, Fused Deposition Modeling with Polypropylene. *Materials & Design* **83**, 768-76 (2015).
33. Faes, Matthias, Eleonora Ferraris, and David Moens, Influence of Inter-Layer Cooling Time on the Quasi-Static Properties of Abs Components Produced Via Fused Deposition Modelling. *Procedia CIRP* **42**, 748-53 (2016).
34. Qattawi, Ala, Buraaq Alrawi, and Arturo Guzman, Experimental Optimization of Fused Deposition Modelling Processing Parameters: A Design-for-Manufacturing Approach. *Procedia Manufacturing* **10**, 791-803 (2017).
35. Fernandez-Vicente, Miguel, Wilson Calle, Santiago Ferrandiz, and Andres Conejero, Effect of Infill Parameters on Tensile Mechanical Behavior in Desktop 3d Printing. *3D Printing and Additive Manufacturing* **3**, 183-92 (2016).

36. Domingo-Espin, Miquel, Salvador Borros, Nuria Agullo, Andres-Amador Garcia-Granada, and Guillermo Reyes, Influence of Building Parameters on the Dynamic Mechanical Properties of Polycarbonate Fused Deposition Modeling Parts. *3D Printing and Additive Manufacturing* **1**, 70-77 (2014).
37. Kishore, Vidya, Christine Ajinjeru, Andrzej Nycz, Brian Post, John Lindahl, Vlastimil Kunc, and Chad Duty, Infrared Preheating to Improve Interlayer Strength of Big Area Additive Manufacturing (Baam) Components. *Additive Manufacturing* **14**, 7-12 (2017).
38. Du, Jun, Zhengying Wei, Xin Wang, Jijie Wang, and Zhen Chen, An Improved Fused Deposition Modeling Process for Forming Large-Size Thin-Walled Parts. *Journal of Materials Processing Technology* **234**, 332-41 (2016).
39. Knoop, F, and V Schoeppner. "Mechanical and Thermal Properties of Fdm Parts Manufactured with Polyamide 12." Paper presented at the Solid Freeform Fabrication Symposium, Austin, 2015.
40. Motaparti, Krishna P, Gregory Taylor, Ming C Leu, K Chandrashekhara, James Castle, and Mike Matlack. "Effects of Build Parameters on Compression Properties for Ultem 9085 Parts by Fused Deposition Modeling." Paper presented at the Solid Freeform Fabrication 2016: Proceedings of the 26th Annual International Solid Freeform Fabrication Symposium, Austin, Texas, USA, 2016.
41. Lee, CS, SG Kim, HJ Kim, and SH Ahn, Measurement of Anisotropic Compressive Strength of Rapid Prototyping Parts. *Journal of materials processing technology* **187**, 627-30 (2007).
42. Upadhyay, Kshitiz, Ravi Dwivedi, and Ankur Kumar Singh. "Determination and Comparison of the Anisotropic Strengths of Fused Deposition Modeling P400 Abs." In *Advances in 3d Printing & Additive Manufacturing Technologies*, 9-28: Springer, 2017.
43. Lužanin, Ognjan, Dejan Movrin, and Miroslav Plančak, Effect of Layer Thickness, Deposition Angle, and Infill on Maximum Flexural Force in Fdm-Built Specimens. *Journal for Technology of Plasticity* **39**, 49-58 (2014).
44. Young, DEVIN, JEFF Kessler, and MICHAEL Czabaj. "Interlayer Fracture Toughness of Additively Manufactured Unreinforced and Carbon-Fiber-Reinforced Acrylonitrile Butadiene Styrene." Paper presented at the 31st Annual Technical Conference of the American Society for Composites, ASC 2016, 2016.
45. Love, Lonnie J, Vlastamil Kunc, Orlando Rios, Chad E Duty, Amelia M Elliott, Brian K Post, Rachel J Smith, and Craig A Blue, The Importance of Carbon Fiber to Polymer Additive Manufacturing. *Journal of Materials Research* **29**, 1893-98 (2014).
46. Yang, Chuncheng, Chuncheng Yang, Xiaoyong Tian, Xiaoyong Tian, Tengfei Liu, Tengfei Liu, Yi Cao, *et al.*, 3d Printing for Continuous Fiber Reinforced Thermoplastic Composites: Mechanism and Performance. *Rapid Prototyping Journal* **23**, 209-15 (2017).
47. Ravi, Abinesh Kurapatti, Anagh Deshpande, and Keng H. Hsu, An in-Process Laser Localized Pre-Deposition Heating Approach to Inter-Layer Bond Strengthening in Extrusion Based Polymer Additive Manufacturing. *Journal of Manufacturing Processes* **24**, 179-85 (2016).
48. Lee, John, and Adam Huang, Fatigue Analysis of Fdm Materials. *Rapid prototyping journal* **19**, 291-99 (2013).
49. Corbett, Taylor, Thijs Kok, C Lee, and J Tarbutton. "Identification of Mechanical and Fatigue Characteristics of Polymers Fabricated by Additive Manufacturing Process." Paper presented at the Proc. 2014 ASPE Spring Topical Meeting: Dimensional Accuracy and Surface Finish in Additive Manufacturing, Berkeley, California, USA, 2014.
50. Ziemian, C. W., R. D. Ziemian, and K. V. Haile, Characterization of Stiffness Degradation Caused by Fatigue Damage of Additive Manufactured Parts. *Materials & Design* **109**, 209-18 (2016).

51. Gomez-Gras, Giovanni, Ramón Jerez-Mesa, J. Antonio Travieso-Rodriguez, and Jordi Lluma-Fuentes, Fatigue Performance of Fused Filament Fabrication Pla Specimens. *Materials & Design* **140**, 278-85 (2018).
52. Jerez-Mesa, R., J. A. Travieso-Rodriguez, J. Llumà-Fuentes, G. Gomez-Gras, and D. Puig, Fatigue Lifespan Study of Pla Parts Obtained by Additive Manufacturing. *Procedia Manufacturing* **13**, 872-79 (2017).
53. Mohamed, Omar Ahmed, Syed Hasan Masood, and Jahar Lal Bhowmik, Experimental Investigation of Creep Deformation of Part Processed by Fused Deposition Modeling Using Definitive Screening Design. *Additive Manufacturing* **18**, 164-70 (2017).
54. ———, Experimental Investigation of Time-Dependent Mechanical Properties of Pc-Abs Prototypes Processed by Fdm Additive Manufacturing Process. *Materials Letters* **193**, 58-62 (2017).
55. Türk, Daniel-Alexander, Franco Brenni, Markus Zogg, and Mirko Meboldt, Mechanical Characterization of 3d Printed Polymers for Fiber Reinforced Polymers Processing. *Materials & Design* **118**, 256-65 (2017).
56. Salazar-Martín, Antonio G., Marco A. Pérez, Andrés-Amador García-Granada, Guillermo Reyes, and Josep M. Puigoriol-Forcada, A Study of Creep in Polycarbonate Fused Deposition Modelling Parts. *Materials & Design* **141**, 414-25 (2018).
57. Mohamed, Omar Ahmed, Syed Hasan Masood, and Jahar Lal Bhowmik, Influence of Processing Parameters on Creep and Recovery Behavior of Fdm Manufactured Part Using Definitive Screening Design and Ann. *Rapid Prototyping Journal* **23**, 998-1010 (2017).
58. Mirzendehdel, Amir M., and Krishnan Suresh, Support Structure Constrained Topology Optimization for Additive Manufacturing. *Computer-Aided Design* **81**, 1-13 (2016).
59. Gaynor, Andrew T., Nicholas A. Meisel, Christopher B. Williams, and James K. Guest. "Topology Optimization for Additive Manufacturing: Considering Maximum Overhang Constraint." In *15th Aiaa/Issmo Multidisciplinary Analysis and Optimization Conference*. Aiaa Aviation Forum: American Institute of Aeronautics and Astronautics, 2014.
60. Thompson, Mary Kathryn, Giovanni Moroni, Tom Vaneker, Georges Fadel, R. Ian Campbell, Ian Gibson, Alain Bernard, *et al.*, Design for Additive Manufacturing: Trends, Opportunities, Considerations, and Constraints. *CIRP Annals* **65**, 737-60 (2016).
61. manufacturing, ISO/TC 261 Additive. "Iso/Astm Dis 52903-1 (Astm F42) Additive Manufacturing -- Standard Specification for Material Extrusion Based Additive Manufacturing of Plastic Materials -- Part 1: Feedstock Materials." International Organization for Standardization, https://www.iso.org/standard/67290.html?browse=tc.
62. Zeltmann, Steven Eric, Nikhil Gupta, Nektarios Georgios Tsoutsos, Michail Maniatakos, Jeyavijayan Rajendran, and Ramesh Karri, Manufacturing and Security Challenges in 3d Printing. *JOM* **68**, 1872-81 (2016).
63. Gajdoš, Ivan, and Ján Slota, Influence of Printing Conditions on Structure in Fdm Prototypes. *Tehnički vjesnik* **20**, 231-36 (2013).
64. Goh, G. D., V. Dikshit, A. P. Nagalingam, G. L. Goh, S. Agarwala, S. L. Sing, J. Wei, and W. Y. Yeong, Characterization of Mechanical Properties and Fracture Mode of Additively Manufactured Carbon Fiber and Glass Fiber Reinforced Thermoplastics. *Materials & Design* **137**, 79-89 (2018).
65. Waller, Jess M, Bradford H Parker, Kenneth L Hodges, Eric R Burke, and James L Walker, Nondestructive Evaluation of Additive Manufacturing State-of-the-Discipline Report. *NASA White Sands Test Facility* (2014).
66. manufacturing, ISO/TC 261 Additive. "Iso/Astm Np 52905 (Astm F42) Additive Manufacturing -- General Principles -- Non-Destructive Testing of Additive Manufactured Products." International Organization for Standardization, https://www.iso.org/standard/71988.html?browse=tc.

67. Kousiatza, Charoula, Nikoleta Chatzidai, and Dimitris Karalekas, Temperature Mapping of 3d Printed Polymer Plates: Experimental and Numerical Study. *Sensors* **17**, 456 (2017).
68. Cummings, Ian, Elizabeth Hillstrom, Rielly Newton, Eric Flynn, and Adam Wachtor. "In-Process Ultrasonic Inspection of Additive Manufactured Parts." Cham, 2016.
69. Wu, Haixi, Yan Wang, and Zhonghua Yu, In Situ Monitoring of Fdm Machine Condition Via Acoustic Emission. *The International Journal of Advanced Manufacturing Technology* **84**, 1483-95 (2016).
70. Kousiatza, Charoula, and Dimitris Karalekas, In-Situ Monitoring of Strain and Temperature Distributions During Fused Deposition Modeling Process. *Materials & Design* **97**, 400-06 (2016).
71. Faes, Matthias, Wim Abbeloos, Frederik Vogeler, Hans Valkenaers, Kurt Coppens, Toon Goedemé, and Eleonora Ferraris, Process Monitoring of Extrusion Based 3d Printing Via Laser Scanning. *arXiv preprint arXiv:1612.02219* (2016).
72. Dinwiddie, Ralph B., Vlastimil Kunc, John M. Lindal, Brian Post, Rachel J. Smith, Lonnie Love, and Chad E. Duty. "Infrared Imaging of the Polymer 3d-Printing Process." Paper presented at the SPIE Sensing Technology + Applications, 2014.
73. Fang, Tong, Mohsen A. Jafari, Stephen C. Danforth, and Ahmad Safari, Signature Analysis and Defect Detection in Layered Manufacturing of Ceramic Sensors and Actuators. *Machine Vision and Applications* **15**, 63-75 (2003).
74. Straub, Jeremy, Initial Work on the Characterization of Additive Manufacturing (3d Printing) Using Software Image Analysis. *Machines* **3**, 55 (2015).
75. Kamoona, Salam Nori, Syed Hasan Masood, and Omar Ahmed Mohamed. "An Investigation on Impact Resistance of Fdm Processed Nylon-12 Parts Using Response Surface Methodology." Paper presented at the AIP Conference Proceedings, 2017.
76. Alvarez, C, L Kenny, C Lagos, F Rodrigo, and Miguel Aizpun, Investigating the Influence of Infill Percentage on the Mechanical Properties of Fused Deposition Modelled Abs Parts. *Ingeniería e Investigación* **36**, 110-16 (2016).
77. Vega, V, J Clements, T Lam, A Abad, B Fritz, N Ula, and Omar S Es-Said, The Effect of Layer Orientation on the Mechanical Properties and Microstructure of a Polymer. *Journal of materials engineering and performance* **20**, 978-88 (2011).
78. Singh Boparai, Kamaljit, Rupinder Singh, and Harwinder Singh, Wear Behavior of Fdm Parts Fabricated by Composite Material Feed Stock Filament. *Rapid Prototyping Journal* **22**, 350-57 (2016).
79. Equbal, A., A. K. Sood, V. Toppo, R. K. Ohdar, and S. S. Mahapatra, Prediction and Analysis of Sliding Wear Performance of Fused Deposition Modelling-Processed Abs Plastic Parts. *Proceedings of the Institution of Mechanical Engineers, Part J: Journal of Engineering Tribology* **224**, 1261-71 (2010).
80. Garg, Harish Kumar, and Rupinder Singh, Comparison of Wear Behavior of Abs and Nylon6—Fe Powder Composite Parts Prepared with Fused Deposition Modelling. *Journal of Central South University* **22**, 3705-11 (2015).
81. Costa, S. F., F. M. Duarte, and J. A. Covas, Thermal Conditions Affecting Heat Transfer in Fdm/Ffe: A Contribution Towards the Numerical Modelling of the Process. *Virtual and Physical Prototyping* **10**, 35-46 (2015).
82. Gurrala, Pavan Kumar, and Srinivasa Prakash Regalla, Part Strength Evolution with Bonding between Filaments in Fused Deposition Modelling. *Virtual and Physical Prototyping* **9**, 141-49 (2014).
83. Torrado, Angel R, Corey M Shemelya, Joel D English, Yirong Lin, Ryan B Wicker, and David A Roberson, Characterizing the Effect of Additives to Abs on the Mechanical Property Anisotropy of Specimens Fabricated by Material Extrusion 3d Printing. *Additive Manufacturing* **6**, 16-29 (2015).

84. Rahman, Kazi Moshiur, Todd Letcher, and Riley Reese. "Mechanical Properties of Additively Manufactured Peek Components Using Fused Filament Fabrication." Paper presented at the ASME 2015 International Mechanical Engineering Congress and Exposition, 2015.
85. Wittbrodt, Ben, and Joshua M. Pearce, The Effects of Pla Color on Material Properties of 3-D Printed Components. *Additive Manufacturing* **8**, 110-16 (2015).
86. Ning, Fuda, Weilong Cong, Jingjing Qiu, Junhua Wei, and Shiren Wang, Additive Manufacturing of Carbon Fiber Reinforced Thermoplastic Composites Using Fused Deposition Modeling. *Composites Part B: Engineering* **80**, 369-78 (2015).
87. Rahim, Tuan Noraihan Azila Tuan, Abdul Manaf Abdullah, Hazizan Md Akil, and Dasmawati Mohamad. "Comparison of Mechanical Properties for Polyamide 12 Composite-Based Biomaterials Fabricated by Fused Filament Fabrication and Injection Molding." Paper presented at the AIP Conference Proceedings, 2016.
88. Miller, Andrew T., David L. Safranski, Kathryn E. Smith, Dalton G. Sycks, Robert E. Guldberg, and Ken Gall, Fatigue of Injection Molded and 3d Printed Polycarbonate Urethane in Solution. *Polymer* **108**, 121-34 (2017).

List of Figures

Figure 1

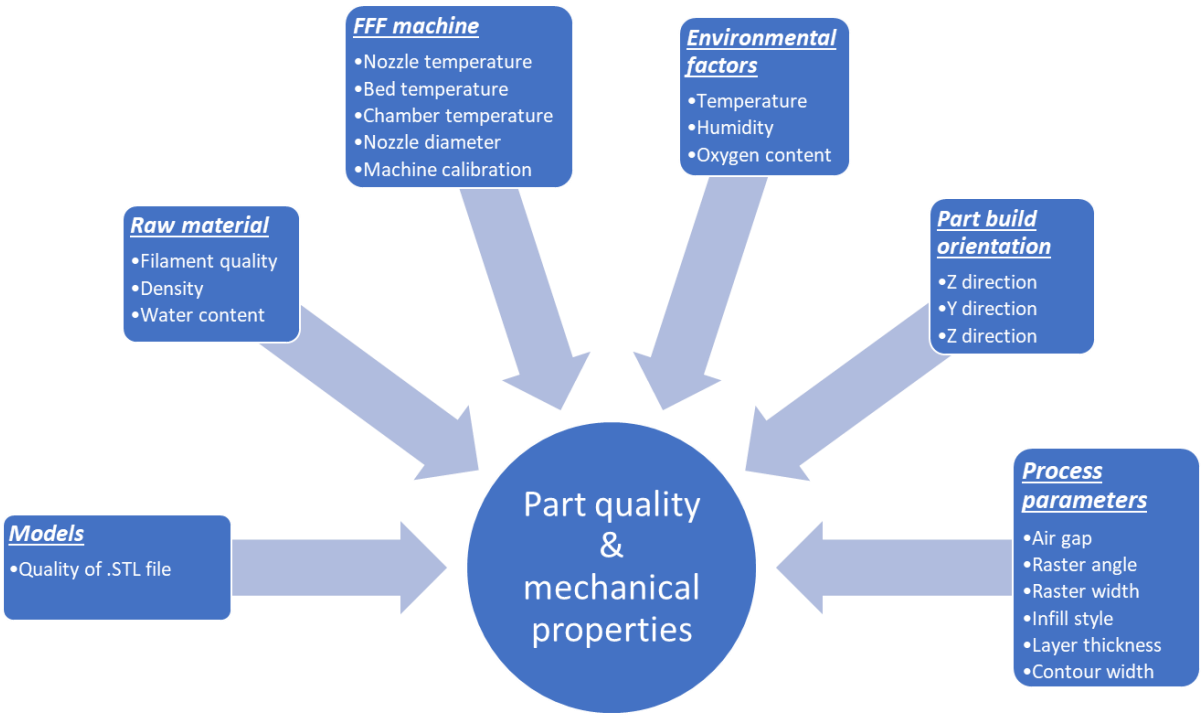
FFF machine
•Nozzle temperature
•Bed temperature
•Chamber temperature
•Nozzle diameter
•Machine calibration
Environmental factors
•Temperature
•Humidity
•Oxygen content
Raw material
•Filament quality
•Density
•Water content
Part build orientation
•Z direction
•Y direction
•Z direction
Models
•Quality of .STL file
Part quality & mechanical properties
Process parameters
•Air gap
•Raster angle
•Raster width
•Infill style
•Layer thickness
•Contour width

Figure 2

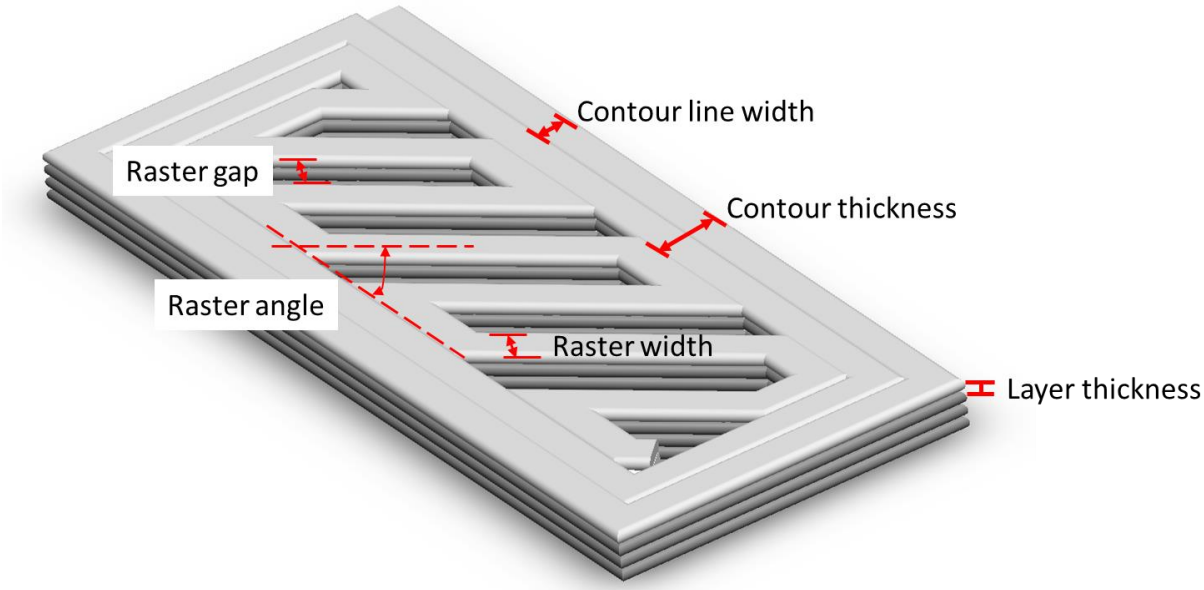
Contour line width
Raster gap
Contour thickness
Raster angle
Raster width
H
Layer thickness

Figure 3

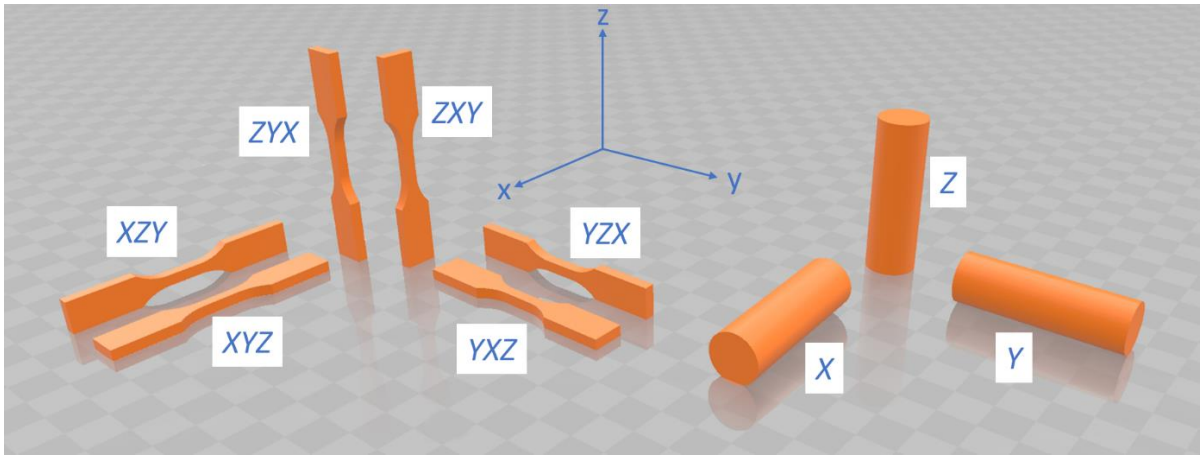

Figure 4

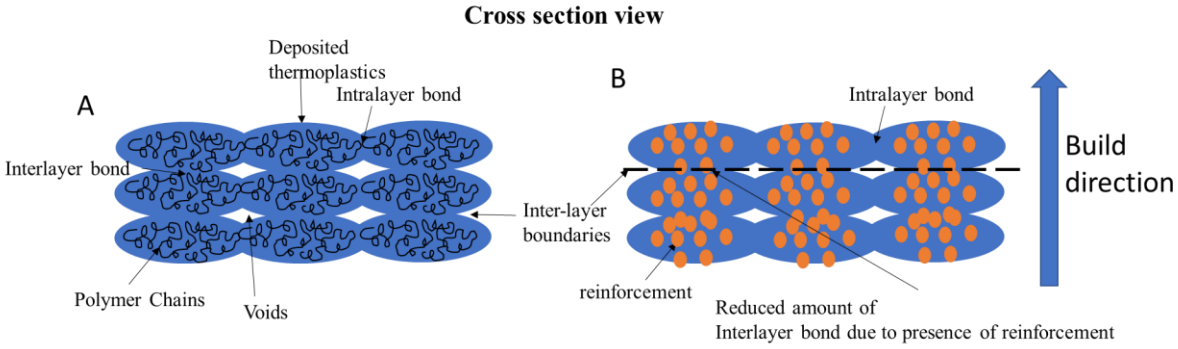
Cross section view
A
Deposited thermoplastics
Intralayer bond
Interlayer bond
Polymer Chains
Voids
Inter-layer boundaries
B
Intralayer bond
Build direction
reinforcement
Reduced amount of Interlayer bond due to presence of reinforcement

Figure 5

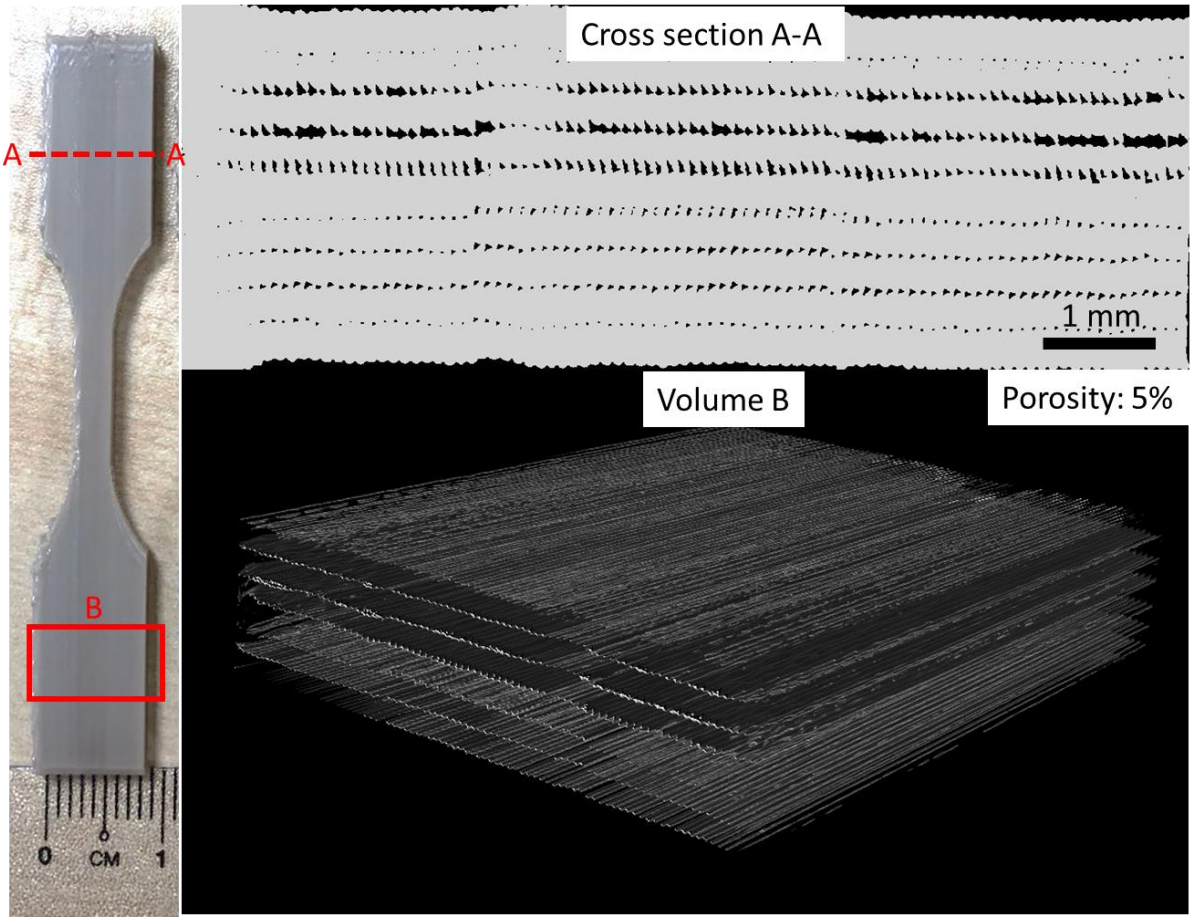

Figure 6

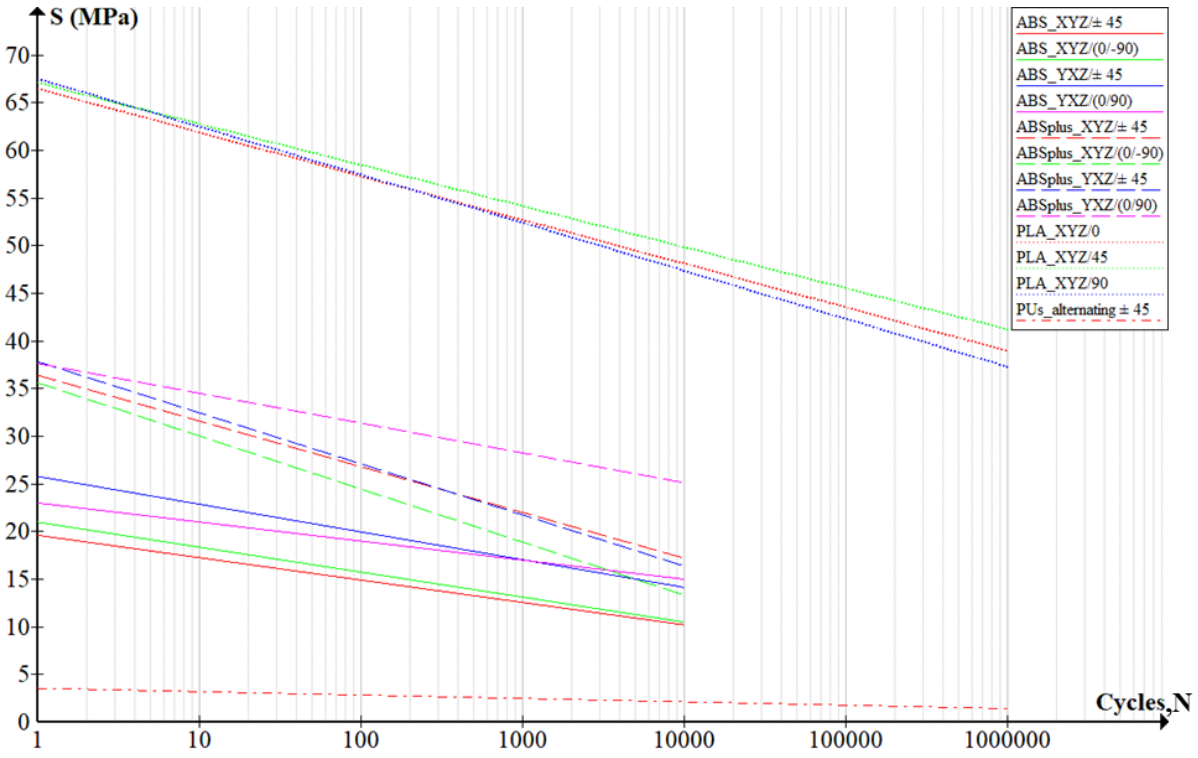
S (MPa)
70
65
60
55
50
45
40
35
30
25
20
15
10
5
0
1
10
100
1000
10000
100000
1000000
Cycles,N
ABS_XYZ/± 45
ABS_XYZ/(0/-90)
ABS_YXZ/± 45
ABS_YXZ/(0/90)
ABSplus_XYZ/± 45
ABSplus_XYZ/(0/-90)
ABSplus_YXZ/± 45
ABSplus_YXZ/(0/90)
PLA_XYZ/0
PLA_XYZ/45
PLA_XYZ/90
PUs_alternating ± 45

Figure 7

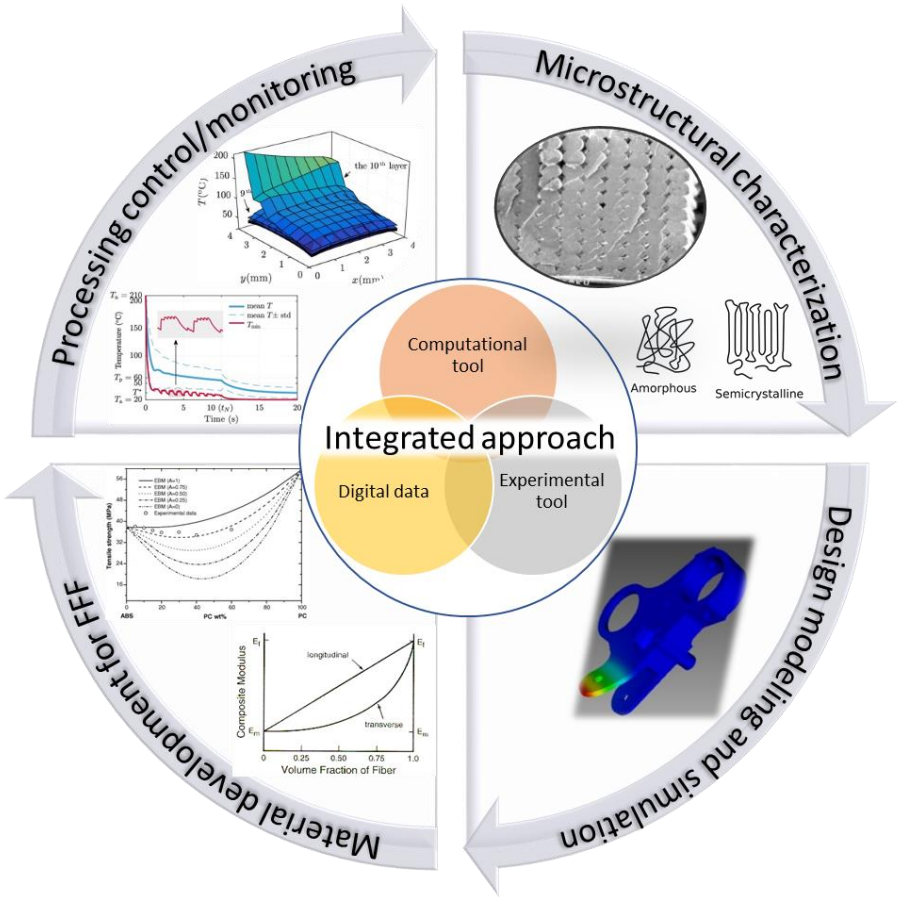
Processing control/monitoring
Microstructural characterization
Design modeling and simulation
Material development for FFF
Computational tool
Integrated approach
Digital data
Experimental tool
Amorphous
Semicrystalline
Time (s)
Volume Fraction of Fiber
Composite Modulus
longitudinal
transverse
ABS
PC
PC wt%

Table 1 Tensile properties

Process	Material	Standard	Sample design	Strain rate/ test setting	Specimen orientation/ raster angle	Layer thickness/ crystallinity	E (GPa)	Yield strength (MPa)	UTS (MPa)	Elongation (%)	Reference
FDM, Printed with heating plate, 100% in-fill	ABS	ASTM D638	Type 1, 0.125”	5 mm/min	XYZ/ 0º		1.2	24	27.6	4.2	[19]
FDM, 100 in-fill,	ABS	ASTM D638	Type V		XYZ/ 0º and 90º		NA	NA	33.96±1.74	8.64±3.3	[83]

				10 mm/min	alternating						
					ZXY/ 0º and 90º alternating		NA	NA	17.73±2.52	2.08±0.55	
FDM, 100% infill, raster angle: 0º, extrusion temperature 340 ºC, platform	PEEK	ASTM D638	Dogbone 165x19x3mm	5 mm/min	XYZ/ 0º		2.871	34.68	71.36	5.01	[84]
					XYZ/ 0º and 90º		2.732	40.40	67.75	3.93	
					XYZ/ 90º		2.846	45.93	53.91	2.29	

temperature: 230 ºC											
FDM, 100% infill,	PLA	ASTM D638	Dogbone 165x19x3mm	50 mm/min	XYZ/ 0º		1.538	NA	38.7	NA	[20]
					YXZ/ 90º		1.246	NA	31.1	NA	
					XYZ/ 45º		1.350	NA	33.6	NA	
FDM, 100% infill	ABS P400	ASTM D638	Dogbone 165.1x19.1x2.5mm	4.46 mm/min	XYZ/0º		1.486	24.18	25.15	NA	[21]
					XYZ/45º		1.042	9.4	10.11	NA	
					XYZ/90º		1.041	8.55	9.16	NA	

					XYZ/45^{o}/ -45 ^{o}		1.282	15.34	16.9	NA	
FDM, 100% infill	PLA	ASTM D638	Dogbone 136.6x19x6mm	5 mm/min	XYZ/0^{o}		3.33	NA	58.45	2.02	[22]
					XYZ/45^{o}		3.60	NA	64.03	2.50	
					XYZ/90^{o}		3.49	NA	54.01	4.14	
FDM, 100% infill Air gap 0.0 mm Nozzle T12 Road width 0.3048 mm	ABS	ASTM D3039	Rectangular slabs 190.5 x 12.7 x 2.6 mm	NA	XYZ/ (0°)		1.549	34.2	38.1	NA	[5]
					XYZ/ (45°)		1.250	221.3	25.7	NA	
					XYZ/ (90°)		1.270	20.8	23.3	NA	
					XYZ/ (+45°/-45°)		1.439	26.5	32.2	NA	

Slice height 0.1778 mm Nozzle temperature 320 ºC Envelope temperature 80 ºC											
FDM, Air gap 0.0mm Nozzle temperature 210 ºC	PLA	ASTM D638-10	Dogbone 165x20x4 mm	2 mm/min	XYZ/0 º	0.06 mm	4.409	NA	88.2	NA	[25]
						0.12 mm	3.892	NA	68.6	NA	
						0.24 mm	3.622	NA	64.6	NA	

					YXZ/0 ^{o}	0.06 mm	4.040	NA	83.4	NA	
						0.12 mm	3.976	NA	65.4	NA	
						0.24 mm	3.934	NA	71.9	NA	
					ZXY/0 ^{o}	0.06 mm	3.266	NA	22.4	NA	
						0.12 mm	3.796	NA	27.5	NA	
						0.24 mm	3.468	NA	39.5	NA	
FDM, 100% infill	PC	ASTM D638	-		**XYZ**/45^{o}/ -45 ^{o}		2.10	45.9	NA	4.35	[24]

				1 mm/min	**YXZ**/45^{o}/-45^{o}		2.41	54.6	NA	4.22	
					ZXY/45^{o}/-45^{o}		2.26	45.6	NA	2.90	
					X+45 ^{o} **Y+45** ^{o} **Z**/45^{o}/-45^{o}		2.13	45.5		3.58	
					Y+45 ^{o} **X+45** ^{o} **Z**/45^{o}/-45^{o}		2.32	53.3		3.35	
					Z+45 ^{o} **X+45** ^{o}		2.18	36		2.05	

					Y/45^{o}/-45^{o}						
FDM, 100% infill, platform temperature: 60 ºC, nozzle temperature: 190 ºC	PLA natural	ASTM 638		NA	ZXY/ 0^{o} and 90^{o} alternating	Crystallinity: 0.93%	NA	52.47	57.16	2.35	[85]
	black					Crystallinity: 2.62%	NA	49.23	52.81	2.02	
	Gray					Crystallinity: 4.79%	NA	46.08	50.84	1.98	
	Blue					Crystallinity: 4.85%	NA	50.10	54.11	2.13	
	White					Crystallinity: 5.05%	NA	50.51	53.97	2.22	
nozzle temperature: 200 ºC						Crystallinity: 4.6%	NA	NA	52.6	NA	

nozzle temperature: 210 ºC						Crystallinity: 13.9%	NA	NA	57.2	NA	
nozzle temperature: 215 ºC						Crystallinity: 5.9%	NA	NA	58.3	NA	
FDM, 100% infill	ABS	ASTM 638		5 mm/min	XYZ	0.2 mm	1.839	29.7	NA	2.01	[27]
						0.3 mm	1.736	27.6	NA	2.31	
						0.4 mm	1.875	28.2	NA	1.97	
	PLA					0.2 mm	3.48	60.4	NA	1.96	
						0.3 mm	3.34	48.5	NA	1.71	

						0.4 mm	3.28 6	54.9	NA	1.94	

Table 2 Compression properties

Technique	Sample design	Material	Strain rate	Specimen orientation/ raster angle	E (GPa)	Yield strength (MPa)	UTS (MPa)	Elongation (%)	Reference
FDM, 100% infill, raster angle: 0°, extrusion temperature: 340 °C, platform	Diameter: 12.7 mm Height: 50.8 mm	PEEK	In accordance to ASTM D695 1.30 mm/min	Z/ 0°	2.035±0.02	66.06±4.41	80.87±2.38	6.65±0.49	[84]
				Z/ 0° and 90°	2.064±0.22	53.67±7.39	72.78±10.51	7.06±1.08	

temperature: 230 ºC									
FDM Layer thickness: 0.2540 mm	Rectangular block: 12.7 x 12.7 x 25.4 mm	ABS	In accordance to ASTM D695 1.30 mm/min	X		32.9±0.36			[42]
				Z		50.1±1.9			
FDM, 100% infill, raster angle: 0º	Diameter: 12.7 mm Height: 25.4	ABS	In accordance to ASTM D695 1.0 mm/min	X/ (45 º /−45 º)	-	-	41	-	[41]
				Z/ (45 º /−45 º)	-	-	38	-	
		ABS		Z/ 0º	0.40264±0.00364	28.83±1.16	32.32±0.58		[5]

FDM, 100% infill, layer height: 0.1778 mm Temperature: 320 ºC	Diameter: 12.7 mm Height: 25.4		In accordance to ASTM D695 1.3 mm/min	Z/ 45 º	0.41720±0.01006	24.46±0.3	33.43±0.20		
				Z/ 90 º	0.38221±0.01031	29.48±0.75	34.69±0.99		
				Z/ (45 º /−45 º)	0.41044±0.01123	28.14±0.64	34.57±0.86		
FDM,	Rectangular block: 38.1 x 38.1 x 25.4 mm	Ultem	1.27mm/min	Z/(0º and 90º)	-	87	-	-	[40]
				X/(0º and 90º)	-	74	-	-	
				Z/ (45 º /−45 º)	-	86	-	-	
				X/ (45 º /−45 º)	-	67	-	-	

Table 3 Flexural properties

Technique	Sample design	Material	Strain rate	Specimen orientation/ raster angle	Layer thickness	E (GPa)	Yield strength (MPa)	UTS (MPa)	Elongation (%)	Reference
FDM, 100% infill, raster angle: 0°, extrusion temperature: 340 °C,	12.7*64*3.2	PEEK	In accordance to ASTM D790 0.01 mm/mm.min	XYZ/ 0°		1.972	86.26	114	10.6	[84]
				XYZ/ 90°		1.954	65.90	83.59	5.81	
				XYZ/ 0° and 90°		2.146	66.50	88.70	6.58	

platform temperature: 230 °C			6.8 mm/min							
FDM, 100% infill, raster angle: 0°	124*12.7*3.2	ABS	1.4 mm/min Support span: 51.2 mm	XYZ		1.75	38	60	3	[86]
FDM, 100% infill, extrusion temperature: 200 °C, layer height 0.3 mm		Nylon	10 mm/min	XYZ/0°/45°/90°/-45°		1.050	-	46	-	[87]

FDM, Air gap 0.0mm Nozzle temperature 210 ºC	65x13x4	PLA	2 mm/min	XYZ/0 º	0.06 mm	1.596	NA	56	NA	[25]
					0.12 mm	1.434	NA	49	NA	
					0.24 mm	1.246	NA	46.2	NA	
				YXZ/0 º	0.06 mm	1.852	NA	65	NA	
					0.12 mm	1.729	NA	61.3	NA	
					0.24 mm	1.886	NA	64.2	NA	
				ZXY/0 º	0.06 mm	1.318	NA	14.3	NA	
					0.12 mm	1.392	NA	23.8	NA	
					0.24 mm	1.414	NA	28.4	NA	
FDM, 100% infill, 230 ºC, platform temperature 65 ºC, extrusion	127x12.7x3.2	PLA	10 mm/min	XYZ/0 º		3.187	NA	102.203	10.6	[22]
				XYZ/45 º		2.985	NA	90.649	7.8	
				XYZ/90 º		3.000	NA	86.136	4.5	

speed 100 mm/s										
FDM, nozzle temperature: 200 °C, printing speed: 20 mm/s, layer height: 0.3 mm,	In accordance to ASTM D790	PA-12	10 mm/min			1376.14	61.27	-	>25	[87]

Table 4 Interlaminar properties

Materials	Sample design	Strain rate/	Specimen orientati	Interlayer properties	Ref-erences

		test setting	on/ raster angle			
ABS	152x22.5x4 Crack length: 76	2 mm/min	XYZ/ 0^{o}	Interlayer fracture toughness (kJ/m^2)	1.57	[44]
ABS with fiber		1 mm/min			0.33	
ABS	ISO 14130:1998 80x10x4 Span length:64mm	NA	XYZ/ 0^{o}	Interlaminar shear (MPa)	24	[46]
ABS with fiber					2.81	
ABS		NA	ZXY	z-direction tensile	16.75± 4.56	[45]

ABS with 13% carbon fiber	ASTM D638 Type V specimens		ZXY		7.00+ 2.59	

Table 5 Fatigue properties

Process	Material	Standard	Sample design	Strain rate/ test setting	Specimen orientation / raster angle	Max cycle stress (MPa)	Stress = A x log(N) +B		Endurance limit	Cycle to failure	Reference
							A	B			
FDM	ABS	UNI EN ISO 527-1 (1997)	10mm by 4mm cross-section with a gauge length of 80mm.	Pulling: 25.4mm/min Relaxing: 12.7mm/min 0.1 Hz	XYZ/± 45	19	-2.35	19.61			[48]
					XYZ/(0/-90)	21	-2.62	20.98			
					YXZ/± 45	25	-2.91	25.78			
					YXZ/(0/90)	23	-2	23.0			
	ABS plus				XYZ/± 45	35	-4.80	36.4			

					XYZ/(0/-90)	36	-5.57	35.6			
					YXZ/± 45	37.5	-5.36	37.82			
					YXZ/(0/90)	37	-3.13	37.64			
					ZXY/± 45	14.5	-1.758	14.8953			
					ZXY/(0/-90)	14.5	-2.12	14.5			
	ABS-P400	ASTM D7791	165.1x19.1x2.5mm	0.25 Hz for 17,5000 cycles	XYZ/0	25.15	-5.94	37.56			[21]
					XYZ/90	9.16	-1.68	11.13			

					XYZ/45	10.11	-2.25	14.03			
					XYZ/± 45	16.9	-4.91	30.5			
	PLA	ASTM D7791	136.6x19x6mm	sinusoidal loading waveform at 2 Hz up to 1,000 cycles, then 5 Hz up to 10,000 cycles and then 20 Hz until failure	XYZ/0	102	-4.59	66.46	5 MPa		[22]
					XYZ/45	90	-4.31	67.07	10 MPa		
					XYZ/90	86	-5.04	67.51	0.5 MPa		

	ABS	ASTM D7774-12	150mm long, 20mm wide and 3mm thick	0.5%	0	35	NA	NA	NA	20000-40000 (drop 10% of originalloa d)	[49]
					90	30				70000-320000	
	polycarbonate urethanes (PCUs)	ASTM E606 and D4482		5 Hz	alternating ± 45	2.2	-0.355	3.56	1.52 and 1.61 MPa		[88]
						4.3	-0.56	5.37	1.79 and 2.33 MPa		

						7	-0.53	6.96	2.87 and 3.63 MPa		